doi: 10.17221/283/2015-VETMED

Evaluation of poly(lactide-co-glycolide)/hydroxyapatite nanofibres for reconstruction of critical-sized segmental bone defects in a canine model

S.Y. Heo[1], H.Y. Kim[2], N.S. Kim[1]*

[1]College of Veterinary Medicine, Chonbuk National University Specialized Campus, Iksan, Republic of Korea

[2]Department of BIN Fusion Technology, Chonbuk National University, Jeonju, Republic of Korea

*Corresponding author: namsoo@jbnu.ac.kr

ABSTRACT: The treatment of segmental bone defects is a challenging problem for both human and veterinary medicine. Various biomaterials have successfully been used to treat these defects. Numerous recent *in vitro* studies have shown the potential of treating bone tissues using poly(lactide-co-glycolide)/hydroxyapatite (PLGA/HAp) nanofibres, which are fabricated using electrospinning. The purpose of this study was to evaluate the possibility of using a bone scaffold of PLGA/HAp nanofibres to repair critical-sized segmental bone defects in a canine model. The experimental bone defects were created in a 15 mm-long region of the radius. The area of the defect in each of 10 Beagle dogs was treated with a transplant of PLGA/HAp nanofibres in gelatin. The control group consisted of five Beagle dogs with similar defect sites that were not treated. Radiological and histological examinations were used to monitor the response of PLGA/HAp nanofibre-treated canine bone. Micro-computed tomography (micro-CT) was used to evaluate bone mass parameters 18 weeks after treatment in the experimental bone defect group. Our radiological and histological results showed that the PLGA/HAp nanofibre is biodegradable in the defect sites and replaces new bone tissue. Micro-CT showed that bone mass parameters were significantly ($P < 0.05$) increased in the critical-sized segmental bone defects of PLGA/HAp nanofibre-treated animals as compared to those of untreated animals. Based on these results, we conclude that PLGA/HAp nanofibres may be used as a bone scaffold biomaterial in canines.

Keywords: poly(lactide-co-glycolide); hydroxyapatite; nanofiber; electrospinning; critical-size canine defect model

The treatment of segmental bone defects is a challenging problem in both human and veterinary medicine (Buma et al. 2004; Reichert et al. 2009). Critical-sized segmental bone defects result from trauma, nonunion, tumour excision, and revision surgery of prosthetic implants (Reichert et al. 2009; Lyu et al. 2013). Various biomaterials have been successfully used to treat segmental bone defects. Of these, autografts, allografts, xenografts, or synthetic graft materials are most popular in clinical orthopaedics (Salgado et al. 2004).

Autografts are good choice for enhancing bone repair and reconstructing critical-sized segmental bone defects because they reliably incorporate and remodel the fracture site (Burg et al. 2000; Buma et al. 2004; Salgado et al. 2004; Reichert et al. 2009). However, autografts are limited by the supply of graft bones and are associated with donor site morbidity, pain, infection, and the possibility of nerve damage (Jose et al. 2009; Jose et al. 2010; Meng et al. 2013). Because of the limitations of autografts, allografts and xenografts are currently used for reconstruction of critical-sized segmental bone defects to provide osteoinduction, osteoconduction, and mechanical strength. However, allografts and xenografts also hold disadvantages: they can trig-

Supported by the Basic Science Research Program through the National Research Foundation of Korea funded by the Ministry of Science, ICT and Future Planning (Grant No. 2013R1A1A2063515).

doi: 10.17221/283/2015-VETMED

ger an immune response and may promote disease transmission (Burg et al. 2000; Buma et al. 2004; Salgado et al. 2004; Reichert et al. 2009; Bhardwaj and Kundu 2010; Yu et al. 2010).

Synthetic graft materials, which use tissue engineering, may be a solution to the problems associated with previously used bone graft materials. The ideal scaffold must be biocompatible, have structural integrity, and act as a temporary framework for the cells in the tissue until the newly formed bone is generated. Additionally, the ideal scaffold must maintain a proper balance between mechanical properties, porous architecture, and degradability, while remaining osteoconductive (Burg et al. 2000; Salgado et al. 2004; Bhardwaj and Kundu 2010).

Electrospun nanofibres have many advantages in bone tissue reconstruction, and are easily produced using synthetic polymers, natural tissues; moreover, they allow for the addition of other materials such as HAp to the polymer backbone. Their wide surface area can promote cell attachment, proliferation, and mineralisation. Moreover, the structure of electrospun nanofibres is similar to that of the natural bone extracellular matrix (Christenson et al. 2007; Smith et al. 2009; Bhardwaj and Kundu 2010; Yu et al. 2010).

Poly(lactide-co-glycolide), an FDA-approved polymer, is a popular biodegradable material characterised by the adjustability of its degradation rate, good mechanical properties, and excellent processability (Pan and Ding 2012). HAp is combined with other polymers to create electrospun nanofibres such as PCL/HAp, Collagen/HAp, and PLLA/HAp, which are the main structural material in the bone (Burg et al. 2000; Buma et al. 2004; Salgado et al. 2004; Bhardwaj and Kundu 2010).

Numerous *in vitro* studies have demonstrated the potential of bone tissue engineering using poly(lactide-co-glycolide)/hydroxyapatite (PLGA/HAp) nanofibres, which is fabricated using electrospinning (Heo et al. 2014; Lipner et al. 2014; Haider et al. 2015; Stachewicz et al. 2015). However, the authors of these *in vitro* reports were unable to assess the biomechanical properties of the bone engineering processes. The purpose of this study was to evaluate the possibility of using a three-dimensional electrospun nanofibrous scaffold of PLGA/HAp nanofibre with gelatin to repair critical-sized segmental bone defects in a canine model. To our knowledge, this is the first report using PLGA/HAp nanofibres to treat critical-sized segmental bone defects in an *in vivo* setting.

MATERIAL AND METHODS

Implants. Poly(lactide-co-glycolide) (PLGA, LA/GA 70/30, MW = 200 kDa) and gelatin (type B, from bovine skin, approximately 225 Bloom) were obtained from Sigma-Aldrich Inc. USA. Synthetic hydroxyapatite ($Ca_3(PO_4)_2$; KT) (Fluka cat. No. 21223, Sigma-Aldrich, UK) was supplied in powdered form. Electrospun PLGA/Haps were prepared as previously reported (Chen et al. 2006; Heo et al. 2014). PLGA was dissolved in methylene chloride and dimethylformamide (Du Pont, USA) at a ratio of 80/20 to obtain a 10 wt% solution. The prepared HAp was added to the 10 wt% solution to create a final mixture containing Hap at 1 wt% solids. Electrospinning was performed with a feed rate of 6 ml/h and applied to 15 kV voltages using a high voltage power supply (CPS-60 K02V1, Chungpa EMT Co., Korea). The distance between the needle tip and the collector was 15 cm. The electrospun nanofibres were dried under vacuum for one week to remove any residual methylene chloride/dimethylformamide and then rolled with 5-mm Steinmann pins and attach to the sheet using methylene chloride/dimethylformamide to make a three-dimensional electrospun nanofibrous scaffold. The custom-made three-dimensional electrospun nanofibrous scaffolds were oval-shaped cylinders with an area of 5 × 10 mm^2 and were 15 mm long with a wall thickness of 2 mm (Figures 1A and 1B). The scaffolds were sterilised with EO gas and stored at room temperature.

Experimental animals and design. Fifteen Beagle dogs (10 intact males and five intact females, mean age 3.6 ± 0.7 years, and mean weight 13.6 ± 2.16 kg) were used in this study. Physical and radiographic examinations were performed to ensure the absence of orthopaedic diseases. The animals were divided into two groups. The experimental group contained 10 Beagle dogs; the defect area in each animal was repaired with a transplant of PLGA/HAp nanofibre with gelatin. The control group consisted of five dogs that were not treated at the defect site. The care and use of the animals reported in this study were approved by the Institutional Animal Care and Use Committee of Chonbuk National University.

Surgical technique. Prior to surgery, each dog received atropine (0.02 mg/kg *s.c.*, Atropine Sulfate Daewon®; Dae Won Pharm, Republic of Korea) and butorphanol (0.3 mg/kg *i.m.*, Butophan Inj®; Myung Moon Pharm, Republic of Korea). General

doi: 10.17221/283/2015-VETMED

anaesthesia was induced with propofol (6 mg/kg *i.v.*, Anepol IN®; Hana Pharm Co. Ltd., Republic of Korea) and was maintained with isoflurane (Forane soln®, JW pharmaceutical, Republic of Korea) delivered in oxygen. Each animal received 25 mg/kg intramuscular cephalexin (Methilexin®, Union Korea Pharm, Republic of Korea) for prophylaxis. Under sterile conditions, each dog was placed in a lateral recumbent position. A skin incision was made at the medial aspect of the radius. For the canine bone defect model, a unilateral 15 mm-long region in the radius diaphysis was created using an oscillating saw under continuous saline irrigation. The bone defects were fixed with a 7-holed LC-DCP plate and 3.5 cortical screws (Figures 1C and 1D) (Synthesis, USA). After the bone defect sites were irrigated with saline solution, the bone defects of the 10 experimental animals were implanted with custom-made three-dimensional (3D) electrospun nanofibrous scaffolds (PLGA/HAp 1 wt%) without fixation, while the bone defects in the five control animals were not treated. The scaffolds were instilled with 2% gelatin before implantation. The surgical incisions were closed in layers. Postoperative treatment consisted of butophanol (Butopan Inj®, Hana Pharm. Co. Ltd., Republic of Korea) administered at a dose of 10 mg/kg *i.m.*, every 12 h for three days and cephalexin (Methilexin Inj®, Union Korea Pharm Co. Ltd., Republic of Korea) 25 mg/kg *i.v.*, every 12 h for four days. Postoperative radiography was obtained for all operated radiuses to ensure adequate implant placement and alignment. Animals were permitted to freely bear weight and eat immediately following surgery. For the first week, the temperature of each animal was recorded, and the canines were observed for orthopaedic symptoms, movement, and appetite. The operation sites were observed for inflammation, infection, swelling, and wound dehiscence.

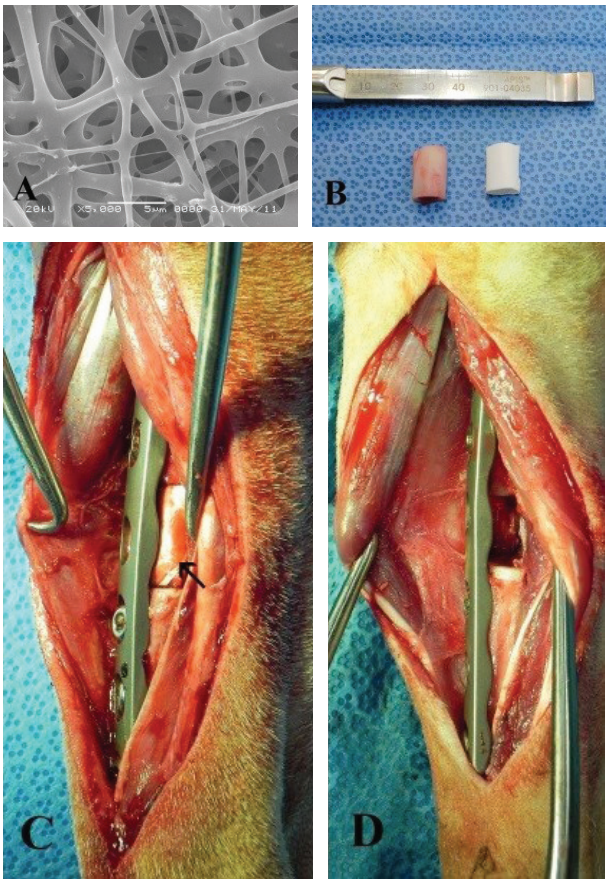

Figure 1. SEM images of electrospun PLGA/HAp nanofibers (**A**), the normal radius (left) and a three-dimensional PLGA/HAp nanofibre (right) (**B**). An intraoperative view of a radius defect. Three-dimensional PLGA/HAp nanofibre with gelatin; radius defect indicated with arrow (**C**), and a 15 mm-long region of radius (**D**)

Haematology and clinical chemistry analysis. Haematology and clinical chemistry analysis were performed on the day of surgery and at 2-week intervals for 36 weeks. Clinical and laboratory assessments for all dogs included a physical examination, a complete blood count performed using an automated animal blood counter (Vet Abc, ABX Diagnostic, Montpellier, France), a blood smear examination, and a basic serum chemistry profile performed using an automated chemistry analyser (Spotchem™ SP-4410, Daiichi Kagaku Co., Japan).

Plain radiography. Radiographs were taken from the right limbs of 10 Beagle dogs treated with three-dimensional electrospun nanofibrous scaffolds, and from the right limbs of five untreated Beagle dogs at 2-week intervals for 18 weeks postoperatively. Periosteal reactions, new bone formation, and remodelling of bone defect sites were evaluated. After 18 weeks, Beagle dogs were euthanized using 0.5 mg/kg of intravenous T61TM (Intervet, Boxmeer, The Netherlands). The right radius was removed, and the soft tissue was harvested *en bloc*. All samples were stored at –45 °C in saline gauze.

Micro-CT. Quantitative evaluation of the bone defect sites was carried out using an X-ray micro-CT instrument (Skyscan in-vivo micro-CT Skyscan n.v., Belgium). The samples were moistened with physiological saline (0.9%) to prevent drying. Scanning at a resolution of 35 µm was performed with an energy of 100 kV and an intensity of 100 µA. Implants were scanned at 180° at 0.4 degree intervals. We used a 0.5 mm aluminium filter to soften

doi: 10.17221/283/2015-VETMED

and even out the X-ray beams. The 2D image slices were reconstructed using a cone beam volumetric algorithm (version 1.8.1.5, CT-analyser Skyscan). The high and low radio-opacity mineralised tissues were differentially segmented using a two-level global thresholding procedure (Gabet et al. 2004). 3D images were made with the software CT-Analyser (Skyscan), and the results of the bone defect sites were evaluated. The following parameters were measured in the 3D model: tissue volume (mm^3); bone volume (mm^3); percent bone volume (%); tissue surface (mm^2); bone surface (mm^2); and bone surface/volume ratio (1/mm).

Histological and histomorphometry examination. Starting 18 weeks prior to euthanasia, animals were given 30 mg/kg body weight of tetracycline. Harvested biopsy tissues were fixed in 10% buffered formalin. The defect sites were observed along the longitudinal section and decalcified as well as undecalcified sections were made. Samples were decalcified with a mixture of formic acid and citric acid. The decalcified samples were embedded in paraffin and sectioned at 5 µm thickness. Each section was stained with haematoxylin and eosin. The sections were examined using light microscopy (Olympus, Japan). The partial undecalcified samples were dehydrated in a graded series of ethanol (70, 80, 90, 95 and 100%) and infiltrated with a mixture of isopropanol and epoxy resin 812; each sample was then embedded in epoxy resin 812 and polymerised in a 60 °C oven for seven days. The polymerised block was cut using a hard tissue cutting machine (Struer Accutom-50, Germany) under constant cooling. The undecalcified sections had an initial thickness of around 150 µm and were successively ground to a thickness of approximately 50 µm using a grinding machine (Struer Rotopol-35, Germany). The sections were examined using fluorescence microscopy (Olympus, Japan). The sections were also examined under a Leica DFC280 light microscope and photographed with a Leica Q Win Plus V3 image analysis system (Leica Microsystems Imaging Solutions, Cambridge, UK) to measure total tissue and bone tissue areas. The area of newly formed bone was measured as a proportion of the total area and calculated as a percentage.

Statistical analyses. The micro-CT data were analysed in an unpaired Student's *t*-test using SAS version 9.1 (SAS Institute Cary, USA). *P*-values of less than 0.05 were considered significant. The data are expressed as mean ± SD.

RESULTS

Surgical follow-up

All dogs tolerated the surgical procedures well, and all fully recovered without infections or additional surgical procedures. The clinical signs of all dogs in this study were within normal ranges. All dogs were able to fully bear weight on the surgical limb.

Haematology and chemical analyses

No significant changes were observed in haematological and clinical chemistry values. The mean white blood cell count and red blood cell profiles (red blood cell, haemoglobin, and haematocrit) of all experimental animals were within the normal range.

Plain radiography

At 12 weeks, X-rays of the experimental group showed new bone formation between the PLGA/HAp nanofibre and the cutting plane of the bone defects. At 18 weeks, the experimental group showed increased new bone formation in the PLGA/HAp nanofibre, but

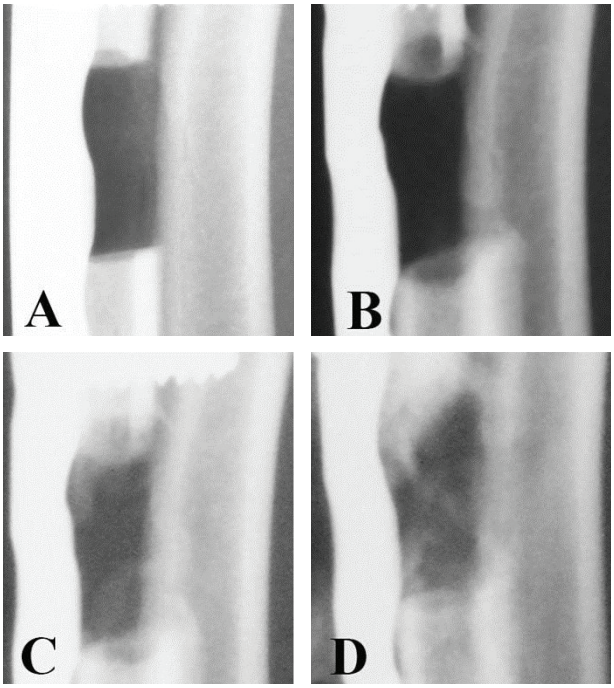

Figure 2. Representative serial radiological images of a radius defect in the experimental group one (**A**), six (**B**), 12 (**C**), and 18 (**D**) weeks post-operatively

doi: 10.17221/283/2015-VETMED

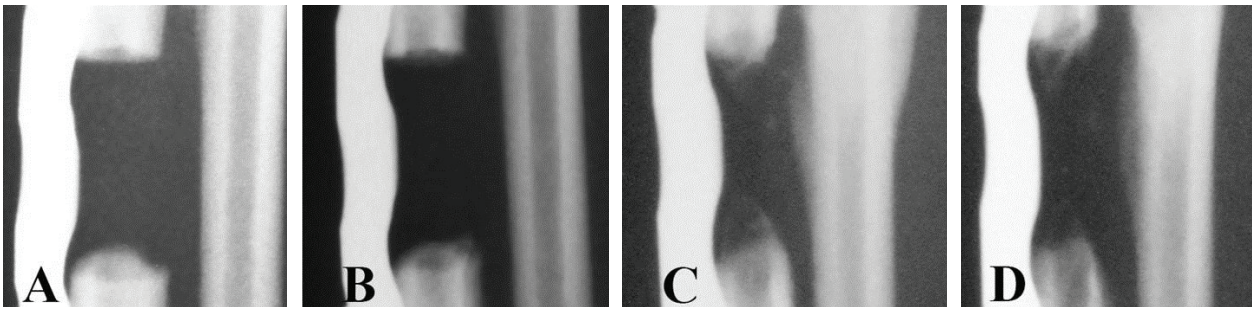

Figure 3. Representative serial radiological images of a radius defect in the control group one (**A**), six (**B**), 12 (**C**), and 18 (**D**) weeks post-operatively

none of the bone defect sites were connected by new bone to the PLGA/HAp nanofibre (Figure 2). In the control group, X-rays showed that there was no new bone formation in the defect site at 18 weeks. The cutting plane of the bone defect responded with a minimal bone reaction in the control group (Figure 3).

Micro-CT

3D-reconstructed micro-CT demonstrated new bone formation in three-dimensional electrospun nanofibrous scaffolds in the experimental group (Figures 4A and 4B). Micro-CT showed that bone

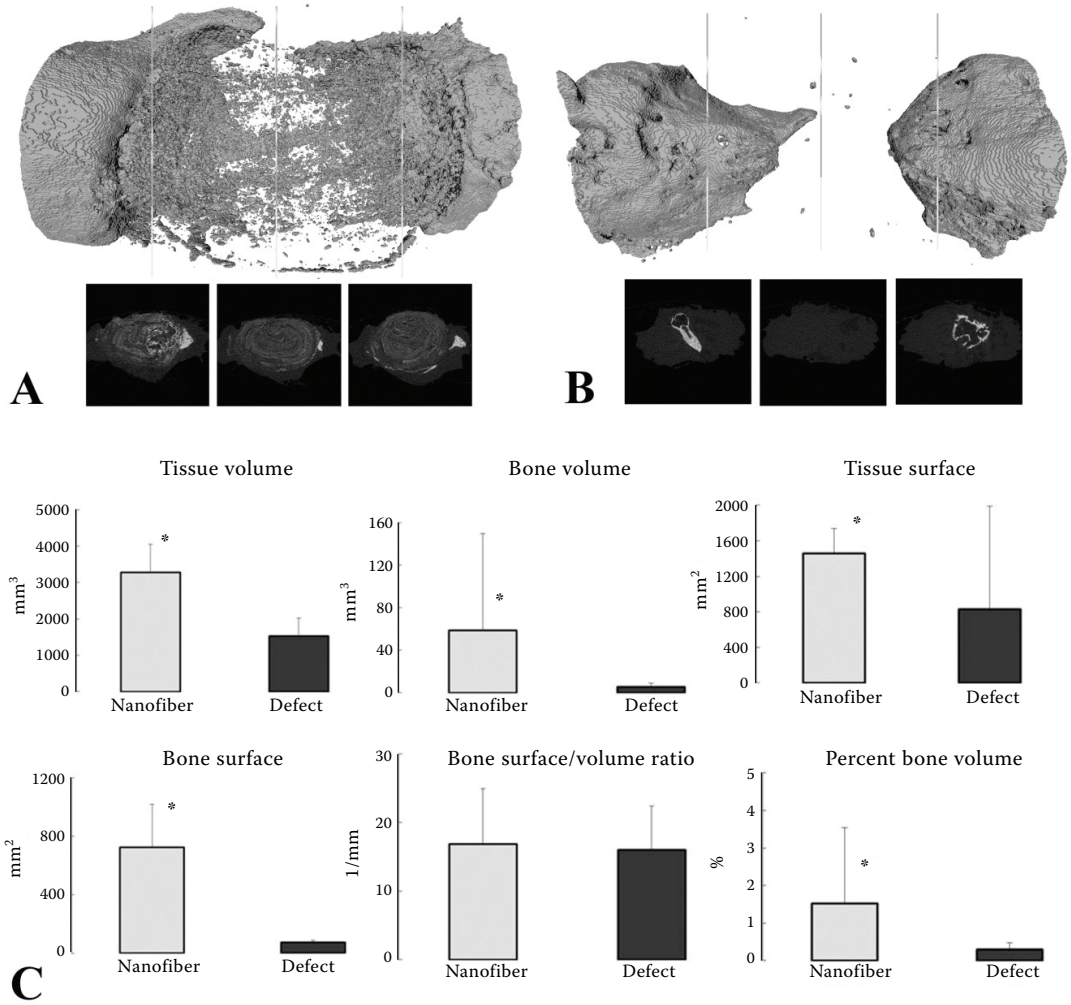

Figure 4. Representative 3D reconstruction micro-CT images 18 weeks after surgery. 3D PLGA/HAp nanofibrous scaffolds with gelatin (**A**), control group (**B**), and bone parameters of 3D micro-CT analysis (*$P < 0.05$) (**C**)

doi: 10.17221/283/2015-VETMED

mass parameters were significantly ($P < 0.05$) increased at the sites of critical-sized segmental bone defects repaired with PLGA/HAp nanofibres with gelatin as compared to untreated sites, except in the case of the bone surface volume ratio. The comparative 3D micro-CT analyses for both groups are shown in Figure 4C.

Histological and histomorphometric results

At 18 weeks, the experimental group showed new bone formation between the PLGA/HAp nanofibre and the cutting plane of the bone defect. There was no inflammatory cell infiltration evident; however, the antra of the bone defects were filled with collagenous connective tissue and the PLGA/HAp nanofibres had degraded. The cutting plane of the bone defect in the experimental group appeared as a yellowish-green fluorescence in fluorescence micrographs (Figure 5E). The histomorphometric results of the experimental group revealed 14% new bone formation and 86% fibrous connective tissue (Figure 5). At 18 weeks, the control group did not show any new bone formation at the bone defect site, but the bone defects were filled with collagenous connective tissue without inflammatory cell infiltration. No fluorescence was seen in the defect site of the control group. The histomorphometric results of the control group revealed 1.4% new bone formation and 98.6% fibrous connective tissue (Figure 6).

DISCUSSION

The results presented in this study demonstrate new bone formation in critical-sized segmental bone defects in a canine model using a three dimensional electrospun nanofibrous scaffold of PLGA/HAp nanofibre with gelatin. Our radiological and histological results showed that PLGA/HAp nanofibres were biodegraded in defect sites and replaced with new bone tissue. Micro-CT analysis of bone mass parameters revealed significant in-

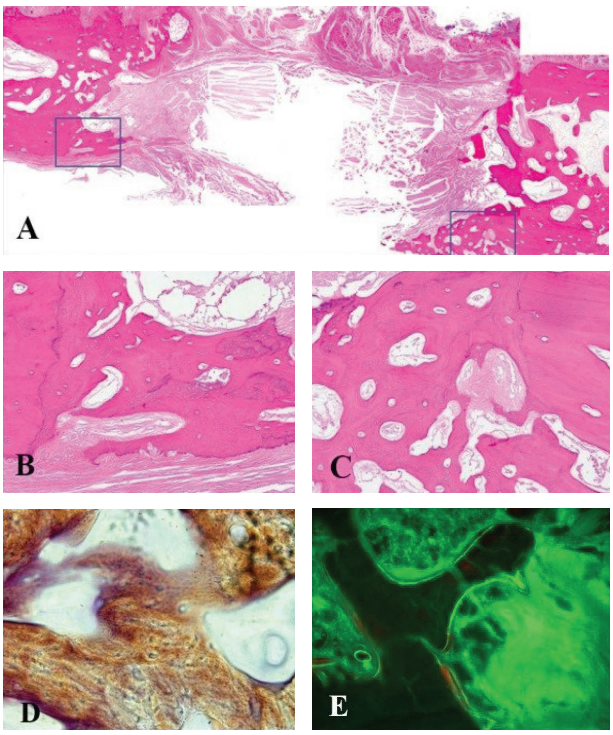

Figure 5. Photomicrographs of the implant site in the group treated with 3D PLGA/HAp nanofibrous scaffolds with gelatin after 18 weeks. The decalcified sections: original magnification × 20 (**A**), original magnification × 100 (**B** and **C**). The undecalcified sections: original magnification × 100 (**D**), fluorescence micrograph original magnification × 100 (**E**)

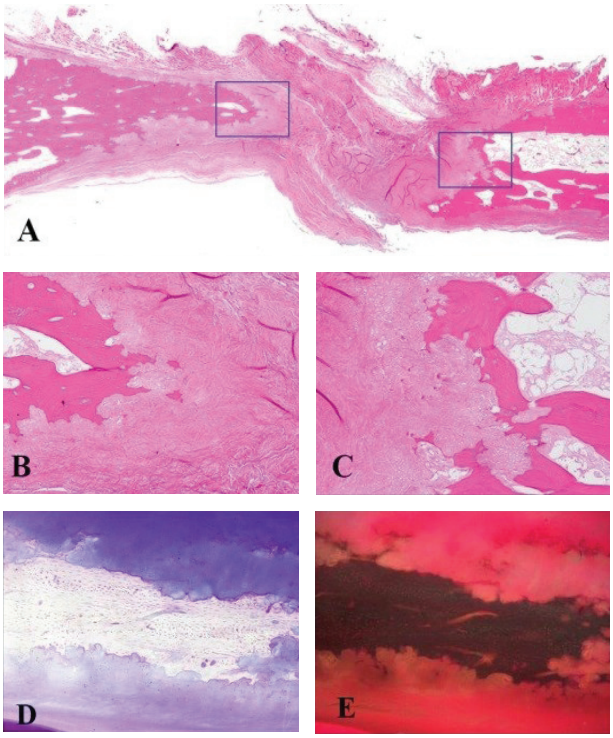

Figure 6. Photomicrographs of the implant site in the control group after 18 weeks. The decalcified sections: original magnification × 20 (**A**), original magnification × 100 (**B** and **C**). The undecalcified sections: original magnification × 100 (**D**), fluorescence micrograph original magnification × 100 (**E**)

doi: 10.17221/283/2015-VETMED

creases ($P < 0.05$) in the critical-sized segmental bone defects repaired with PLGA/HAp nanofibres as compared to untreated sites. Although in a previous study, PLGA with willemite (Zn_2SiO_4) ceramics was investigated for bone reconstruction in calvarial critical-sized defects using a rat model (Adegani et al. 2014), to our knowledge, there has not been an *in vivo* study using three-dimensional electrospun nanofibrous scaffolds of PLGA/HAp nanofibres with gelatin to treat critical-sized segmental bone defects in a canine model.

In bone tissue-engineering nanofibrous scaffolds mimic the natural extracellular matrix and provide for the attachment, proliferation, and differentiation of cells (Smith et al. 2009; Bhardwaj and Kundu 2010). In our previous study conducted to assess cell adhesion to PLGA/HAp nanofibres with gelatin, we identified PLGA/HAp nanofibres in 1% and 2% gelatin that were counterstained with haematoxylin, indicating cell adhesion to the nanofibres, and demonstrating that gelatin is suitable for use for cell adhesion to electrospun nanofibres (Heo et al. 2014). Previous studies with PLGA/HAp nanofibres have attempted to assess cell seeding and viability. Lao et al. (2011) studied PLGA nanofibrous composite scaffolds containing nano-hydroxyapatite particles by electrospinning. In this study, the viability of osteoblasts on PLGA/HAp showed a similar tendency and was dependent on the duration of culture. Cells cultured on PLGA/HAp 5 wt% nanofibres showed significantly higher ALP activity than those cultured on the control PLGA nanofibre. Lao et al. concluded that integration of HAp with the PLGA nanofibres is an effective method of obtaining nanofibrous scaffolds with better physical and biological performance (Lao et al. 2011). In another study on the mechanical characterisation and biodegradation of low concentrations of HAp in PLGA nanofibres, no agglomerates were found but good dispersion was achieved (Jose et al. 2009). However, higher concentrations of HAp resulted in agglomeration, which led to increased diameters and broken fibres. *In vitro* biodegradation characteristics of PLGA/HAp showed similar results, although the neat PLGA and PLGA/HAp 1 wt% showed the lowest absorption and mass loss (Jose et al. 2009).

Electrospun nanofibres have high porosities and surface-area-to-volume ratios. Previous studies have reported that the optimal pore size of nanofibres for a growing cell is between 100 and 500 μm (Yu et al. 2010). HAp has been studied in combination with several natural and synthetic polymers. Nanocomposite scaffolds exhibit better porosity, degradability, and mechanical properties when compared to pure HAp scaffolds. Porosities greater than 90% are possible in composite scaffolds, whereas those in HA scaffolds are usually less than 70% (Smith et al. 2006). However, Jose et al. reported that in PLGA/HAp nanofibres, random PLGA fibres had a 77% porosity, whereas aligned nanofibres had 72% porosity. The porosity of the scaffolds decreased from 72% for neat PLGA to around 62% at nano-HA concentrations of 1%, 5%, and 10% (Jose et al. 2009) as a result of the electrospun nanofibres being incorporated into the hydroxyapatite nanoparticles.

Bone defects treated with the three-dimensional electrospun nanofibrous scaffold of PLGA/HAp nanofibres with gelatin were not completely filled by new bone formation. We did not include osteogenesis factor together with the PLGA/HAp nanofibres in this study. Recent attempts to use PLGA/HAp nanofibres combined with osteogenesis factor have met with varying success. Haider et al. compared a BMP-g-nHA/PLGA hybrid nanofibre scaffold with PLGA nanofibre; they showed that BMP-2 on BMP-g-nHA/PLGA hybrid nanofibre scaffolds greatly stimulated osteoblastic cell growth, compared to the nHA/PLGA and pristine PLGA nanofibre scaffold, which they used as the control (Haider et al. 2015).

Our scaffolds were made using three-dimensional electrospun nanofibrous material. This structure may stimulate the attachment, proliferation, and differentiation of cells. Wang et al. developed nanofibre-containing spiral scaffolds, which are made using poly(ε-caprolactone) (PCL). They demonstrated that these spiral-structured PCL fibrous scaffolds significantly enhanced osteogenic proliferation and differentiation when compared to traditional cylindrical scaffolds used in bone tissue engineering (Wang et al. 2010).

The purpose of our study was to evaluate the possibility of using three-dimensional electrospun nanofibrous scaffolds of PLGA/HAp nanofibres with gelatin for the repair of critical-sized segmental bone defects in a canine model. Our results showed that the PLGA/HAp nanofibres are biodegradable and replace new bone tissue in the defect sites. Comparative 3D micro-CT analysis of healing at the defect sites revealed significantly better values ($P < 0.05$) in the critical-sized segmental bone defects treated with the PLGA/HAp nanofibres. Based on these results,

doi: 10.17221/283/2015-VETMED

we suggest that PLGA/HAp nanofibres can be used as a bone scaffold biomaterial in canines.

REFERENCES

Adegani JF, Langroudi L, Ardeshirylajimi A, Dinarvand P, Dodel M, Doostmohammadi A, Rahimian A, Zohrabi P, Seyedjafari E, Soleimani M (2014): Coating of electrospun poly(lactic-co-glycolic acid) nanofibers with willemite bioceramic: improvement of bone reconstruction in rat model. Cell Biology International 38, 1271–1279.

Bhardwaj N, Kundu SC (2010): Electrospinning: a fascinating fibre fabrication technique. Biotechnology Advances 28, 325–347.

Buma P, Schreurs W, Verdonschot N (2004): Skeletal tissue engineering-from in vitro studies to large animal models. Biomaterials 25, 1487–1495.

Burg KJ, Porter S, Kellam JF (2000): Biomaterial developments for bone tissue engineering. Biomaterials 21, 2347–2359.

Chen J, Chu B, Hsiao BS (2006): Mineralization of hydroxyapatite in electrospun nanofibrous poly(L-lactic acid) scaffolds. Journal of Biomedical Materials Research Part A 79, 307–317.

Christenson EM, Anseth KS, van den Beucken JJ, Chan CK, Ercan B, Jansen JA, Laurencin CT, Li WJ, Murugan R, Nair LS, Ramakrishna S, Tuan RS, Webster TJ, Mikos AG (2007): Nanobiomaterial applications in orthopaedics. Journal of Orthopaedic Research 25, 11–22.

Gabet Y, Muller R, Regev E, Sela J, Shteyer A, Salisbury K, Chorev M, Bab I (2004): Osteogenic growth peptide modulates fracture callus structural and mechanical properties. Bone 35, 65–73.

Haider A, Kim S, Huh MW, Kang IK (2015): BMP-2 grafted nHA/PLGA hybrid nanofibre scaffold stimulates osteoblastic cells growth. BioMed Research International, doi: 10.1155/2015/281909.

Heo SY, Seol JW, Kim NS (2014): Characterisation and assessment of electrospun Poly/hydroxyapatite nanofibres together with a cell adhesive for bone repair applications. Veterinarni Medicina 59, 498–501.

Jose MV, Thomas V, Johnson KT, Dean DR, Nyairo E (2009): Aligned PLGA/HA nanofibrous nanocomposite scaffolds for bone tissue engineering. Acta Biomaterialia 5, 305–315.

Jose MV, Thomas V, Xu Y, Bellis S, Nyairo E, Dean D (2010): Aligned bioactive multi-component nanofibrous nanocomposite scaffolds for bone tissue engineering. Macromolecular Bioscience 10, 433–444.

Lao L, Wang Y, Zhu Y, Zhang Y, Gao C (2011): Poly(lactide-co-glycolide)/hydroxyapatite nanofibrous scaffolds fabricated by electrospinning for bone tissue engineering. Journal of Materials Science: Materials in Medicine 22, 1873–1884.

Lipner J, Liu W, Liu Y, Boyle J, Genin GM, Xia Y, Thomopoulos S (2014): The mechanics of PLGA nanofibre scaffolds with biomimetic gradients in mineral for tendon-to-bone repair. Journal of the Mechanical Behavior of Biomedical Materials 40, 59–68.

Lyu S, Huang C, Yang H, Zhang X (2013): Electrospun fibres as a scaffolding platform for bone tissue repair. Journal of Orthopaedic Research 31, 1382–1389.

Meng ZX, Li HF, Sun ZZ, Zheng W, Zheng YF (2013): Fabrication of mineralized electrospun PLGA and PLGA/gelatin nanofibres and their potential in bone tissue engineering. Materials Science and Engineering C 33, 699–706.

Pan Z, Ding J (2012): Poly(lactide-co-glycolide) porous scaffolds for tissue engineering and regenerative medicine. Interface Focus 2, 366–377.

Reichert JC, Saifzadeh S, Wullschleger ME, Epari DR, Schutz MA, Duda GN, Schell H, van Griensven M, Redl H, Hutmacher DW (2009): The challenge of establishing preclinical models for segmental bone defect research. Biomaterials 30, 2149–2163.

Salgado AJ, Coutinho OP, Reis RL (2004): Bone tissue engineering: state of the art and future trends. Macromolecular Bioscience 4, 743–765.

Smith IO, McCabe LR, Baumann MJ (2006): MC3T3-E1 osteoblast attachment and proliferation on porous hydroxyapatite scaffolds fabricated with nanophase powder. Journal of International Journal of Nanomedicine 1, 189–194.

Smith IO, Liu XH, Smith LA, Ma PX (2009): Nanostructured polymer scaffolds for tissue engineering and regenerative medicine. Wiley Interdisciplinary Reviews: Nanomedicine and Nanobiotechnology 1, 226–236.

Stachewicz U, Qiao T, Rawlinson SC, Almeida FV, Li WQ, Cattell M, Barber AH (2015): 3D imaging of cell interactions with electrospun PLGA nanofibre membranes for bone regeneration. Acta Biomaterialia 27, 88–100.

Wang J, Valmikinathan CM, Liu W, Laurencin CT, Yu X (2010): Spiral-structured, nanofibrous, 3D scaffolds for bone tissue engineering. Journal of Biomedical Materials Research Part A 93, 753–762.

Yu NY, Schindeler A, Little DG, Ruys AJ (2010): Biodegradable poly(alpha-hydroxy acid) polymer scaffolds for bone tissue engineering. Journal of Biomedical Materials Research Part B: Applied Biomaterials 93, 285–295.

Received: December 30, 2015
Accepted after corrections: December 14, 2016